



Thickness measurement via local ultrasonic resonance spectroscopy

Janez Rus^{*}, Christian U. Grosse

Chair of Non-Destructive Testing, Centre for Building Materials, Technical University of Munich, Franz-Langinger-Straße 10, 81245 Munich, Germany

ARTICLE INFO

Keywords:

Local ultrasonic resonance spectroscopy
Local resonance
Thickness resonance
Thickness measurement
Laser-ultrasonics

ABSTRACT

Local ultrasonic resonance spectroscopy (LURS) is a new approach to material inspection, where the specimen is locally excited by a short mechanical impulse while its local mechanical response is recorded at a position nearby. The local material and geometrical properties can be extracted from the frequency spectrum of the response and visualized by performing a scan over the inspected area. In our experiment, the plate thickness and the reliefs of both plate surfaces (plate curvature) were obtained from thickness resonance and time of arrival analysis without physical contact to the specimen. Ultrasound was generated on the specimen surface by a laser pulse. Local mechanical response of a carbon fiber-reinforced polymer plate with a thickness ranging from 0.6 mm to 4.3 mm was recorded with a broadband optical microphone in through-transmission setup. The precision of this arrangement greatly exceeded the precision of conventional methods limited by the ultrasound wavelength. For thicknesses in the range around 1 mm, standard deviations of up to several μm were achieved. An influence of the through-plate ultrasound velocity on the measured relief of the plate surface nearest to the optical microphone was eliminated by a joint evaluation of thickness resonance and time of arrival. Furthermore, we demonstrated that internal delaminations have an influence on the spectrum of the local mechanical response and can therefore be detected by LURS.

1. Introduction

Thickness measurement of plate-like structures, typically performed by observing time-of-flight of transmitted or reflected ultrasound (US) is a routine non-destructive testing task [1,2]. The prevalent piezoelectric generation of US is normally restrained to a relatively narrowband testing frequency, which should be high-enough to achieve adequate resolution. The burst signal length should also be sufficiently short to distinguish the single in-plate reflections. Ideally, a single US pulse is generated. Its length has a lower limit due to the unavoidable compromise between the pulse length (US bandwidth) and pulse energy that can still be effectively detected. Below a certain plate thickness, which depends on the pulse length, the single in-plate US reflections can no longer be distinguished, and the thickness cannot be efficiently determined.

However, in the present research we use a different approach that also delivers convenient results for thinner plates. Instead of studying the wave propagation in the plate, the same elastomechanic problem is addressed using vibration analysis, where the motion is considered integrally through the entire plate thickness. The plate, locally excited by a US pulse, responds with its natural mechanical oscillations. From

the frequency spectrum obtained, the thickness resonance (TR) is typically pronounced in a certain frequency range. By inverting the TR frequency, the period of in-plane reflections is obtained. The plate thickness can be obtained from this period, given the pressure wave velocity or the thickness at a reference point.

We would like to emphasize that for inhomogeneous materials, this thickness can differ locally from the true (geometrical) thickness. Thus, the TR frequency can also be used as a criterion to detect deviations in the material properties if the plate thickness is known, perfectly constant or measured simultaneously. LURS (local ultrasonic resonance spectroscopy) is a broader term to designate the method for inspection of the local geometric and material properties by analyzing the local natural mechanical response [3].

In order to precisely determine the local mechanical properties of the specimen, two conditions for natural oscillations of the localized inspected area need to be met. Firstly, the motion needs to be induced over a broad frequency range (e.g. by short impulse), while the setup should be capable of broadband detection. Secondly, the excitation and detection units should be mechanically detached to ensure free vibration of the specimen.

These conditions were realized by the recently developed

^{*} Corresponding author.

E-mail addresses: janez.rus@tum.de (J. Rus), grosse@tum.de (C.U. Grosse).

<https://doi.org/10.1016/j.ultras.2020.106261>

Received 19 February 2020; Received in revised form 29 August 2020; Accepted 18 September 2020

Available online 23 September 2020

0041-624X/© 2020 Elsevier B.V. All rights reserved.

experimental equipment used for our study. Effective laser-based US generation combined with broadband (several kHz to several MHz) and contact-free US detection facilitates the analysis of the motion in the US frequency range with an approach similar to vibration and modal analysis, which was formerly limited to the lower frequency range. With the shift to higher frequencies, the form of the motion depends predominantly on the local mechanical properties of the specimen. Local resonances of US are acquired from the frequency spectrum of the captured signal. While performing a LURS scan, it is possible to obtain material, geometrical and other mechanical properties for each scanning-grid location, or to detect their spatial change. Some of the measured properties are exclusive – e.g. plate thickness and US velocity in the plate cannot be obtained simultaneously from the TR, if it is considered as a single parameter. If the entire US amplitude spectrum is analyzed together with its phase (or ToA) additional local properties in the scanned region can be obtained.

We considered the properties of the plate integrally across its thickness, while assuming constant US wave velocities in this direction. The assumption of homogeneity of the plate material could be a potential source of error. However, the error was small for the relevant frequency range (up to 2.26 MHz). The corresponding wavelengths were greater than approximately 1 mm for P-waves (and greater than approximately 0.5 mm for S-waves) in the plate material. This exceeded the diameter of the embedded carbon fibers by several orders of magnitude. Influence of the alternating orientation of fiber layers in the plate material (described in Section 2, ‘Experimental methods’) on the obtained results was not distinguishable in our experiment. The thinnest part of the plate consisted of more than two orthogonal fiber layers.

Analyzing the broadband spectrum of the recorded signal, frequency domain B-scans gain a great deal of significance. In the growing field of broadband US inspection, it is advantageous to refer to these as S-scans (spectrum scans).

Only a few experiments applying US spectrum analysis for determining the plate thickness without physical contact to the specimen have been realized. With air-coupled ultrasound (ACU) transducers, it is challenging to achieve the US frequency range required for the spectral analysis. However, electrostatic (or capacitance) transducers are a possible alternative to generate and detect US with a broader frequency range than piezoelectric transducers [4–6]. They were used to determine thickness resonances for up to four different thicknesses of aluminum [4], wood [5], and steel plates [6] in through-transmission setup.

High-energy, short-lasting US pulses can be efficiently generated via laser pulse [7–10]. In combination with a laser interferometer, one longitudinal and two shear resonance frequencies and their high-order resonances were detected [11]. From their peak values, crystallographic properties and thickness of the metal sheet were obtained. The second application used a similar type of US generation and detection to determine the thickness of glass bottles from TR frequency peak [12]. Furthermore, US velocities and elastic constants have been measured for samples with known thicknesses [13]. Using a laser-based through-transmission setup, time delays of in-specimen reflections have been determined by a signal cross-correlation.

In previous contact-free methods to measure plate thickness, US was either generated and detected in air [4–6] or generated and detected by a laser on the specimen surface [11,12]. Contrary to this, in our experiment, US was generated on the specimen surface by a laser pulse and detected by an air-coupled optical microphone. Detection of the (on the surface generated) US in air has the advantage that the ToA of the wave train represents an additional measurable parameter, which is not equivalent to the in-plate reflection period. The position of the specimen is unknown for fully-ACU methods, or when US is generated and detected on the specimen surface. Contrary to this, our hybrid method delivers the surface reliefs of both sides of the plate in the scanned region together with the plate thickness. Curvature of the specimen plate can thus also be measured and discerned from the thickness change with a single measurement.

Effective detection of broadband ultrasound is conditioned by the reflectivity of the surface when using a laser interferometer with the probe laser directed at the surface of the specimen. This can cause distortions when performing a scan. Repeatability of the US detection is an additional advantage when using an air-coupled laser-based optical microphone instead. Compared to previous methods, a higher spatial resolution was achieved while performing a scan over the plate of variable thickness. The thickness was obtained more precisely via TR in a broader US frequency range, when measured simultaneously with surface reliefs.

2. Experimental methods

The test specimen was a 30 × 30 cm carbon fiber reinforced polymer (CFRP) plate (Fig. 1). The plate was constructed with fifteen carbon fiber layers (0°, 90° alternating orientation) each having a thickness of 0.27 mm [14]. Epoxy resin was used as the matrix. The scanned area is marked with a white frame. The thickness of the unmachined plate (scan area excluding the channels) varied between 3.6 mm and 4.3 mm.

The scan was conducted over the area that contained two 10-mm-wide channels machined (milling process) into the CFRP plate (termed *grooves*). The milling depth increased for the higher scanning position x values. The remaining thickness of the plate varied continuously between 33 mm and 43 mm scanning position y (*continuous groove*), and discretely between 3 mm and 13 mm scanning position y (*discrete groove*).

The plate thickness of the continuous groove ranged from 4.05 mm to 0.6 mm, providing a linear decrease for the higher scanning position x values. There was a 0.25 mm step to the full thickness of the plate at the left most side of the continuous groove (scanning position $x = 13$ mm).

The plate thickness of the discrete groove ranged from 3.9 mm to 0.6. Each 0.3-mm discrete thickness change was 12 mm long. There was a 0.4 mm step to the full thickness of the plate at the left most side of the discrete groove (scanning position $x = 7$ mm). Red lines mark the cross-sectional locations in the area of discretely and continuously changing thickness, on which detailed LURS analysis was performed in B-scans in the time and frequency domains (S-scans). The grooved side (shown in Fig. 1) is defined as the rear side of the plate.

An Nd-YAG frequency-doubled, q-switched pulse laser with a wavelength of 532 nm was used to generate the US blast waves in the specimen. The maximum laser pulse repetition rate was 20 Hz. The laser light was collimated to 8-mm diameter w (95% intensity level). Due to the large laser beam diameter, the US was excited in the thermoelastic regime.

In order to detect the TR of plates with varying thickness, a broadband US source needs to be combined with a broadband US detector. We used an Eta450 Ultra optical microphone, manufactured by Xarion Laser Acoustics. The optical microphone does not have any moving parts, since these would inevitably have their own natural mechanical behavior. The US is measured directly in air by measuring the change of refractive index as the acoustic waves travel through the Fabry-Pérot etalon [15–18]. The housing of the microphone or the etalon mirrors may, however, exhibit its own natural behavior, potentially altering the signal. The optical microphone has a frequency range from several kHz to approx. 3 MHz, as obtained by our experiment. Its sensitivity is 100 mV/Pa and it has a self-noise of 10 mPa (full bandwidth) as specified by the manufacturer.

The US source and detector were arranged in a through-transmission setup (Fig. 2) with the laser illuminating the even side of the plate (opposite from the side shown in Fig. 1). The sensitive part (Fabry-Pérot etalon) of the optical microphone was aligned centrally with the axis of the laser beam, approx. 4-mm from the specimen plate (as measured from its full thickness). As the plate thickness varied, the etalon-to-specimen distance changed, while the distance to the laser output optic remained approximately the same.

All of the results described in this work were obtained by a single 13-

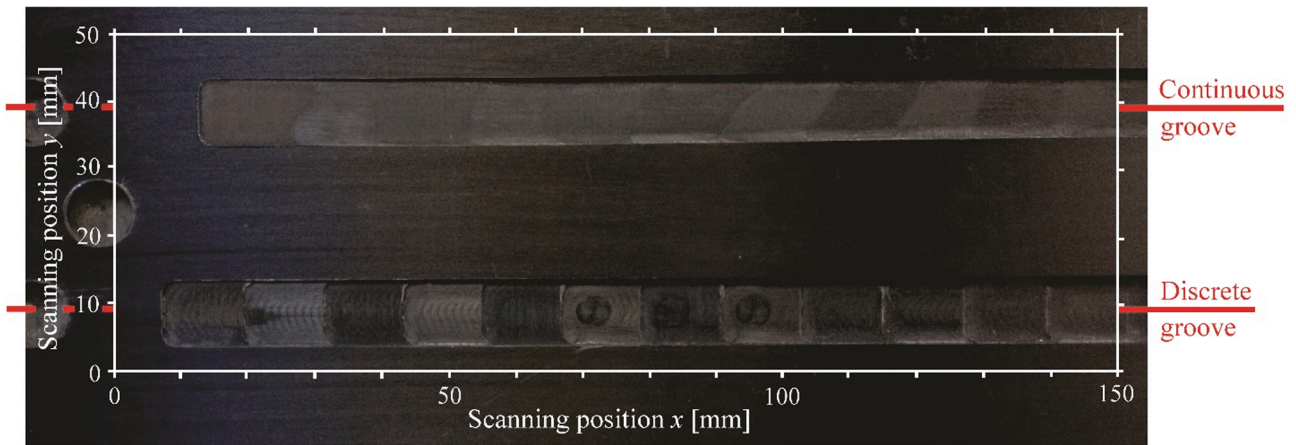


Fig. 1. Rear side of the specimen plate with two grooves, where the plate thickness changes continuously and discretely. The white frame with the coordinate system denotes the scan area. A part of a flat-bottom hole is included in the scan.

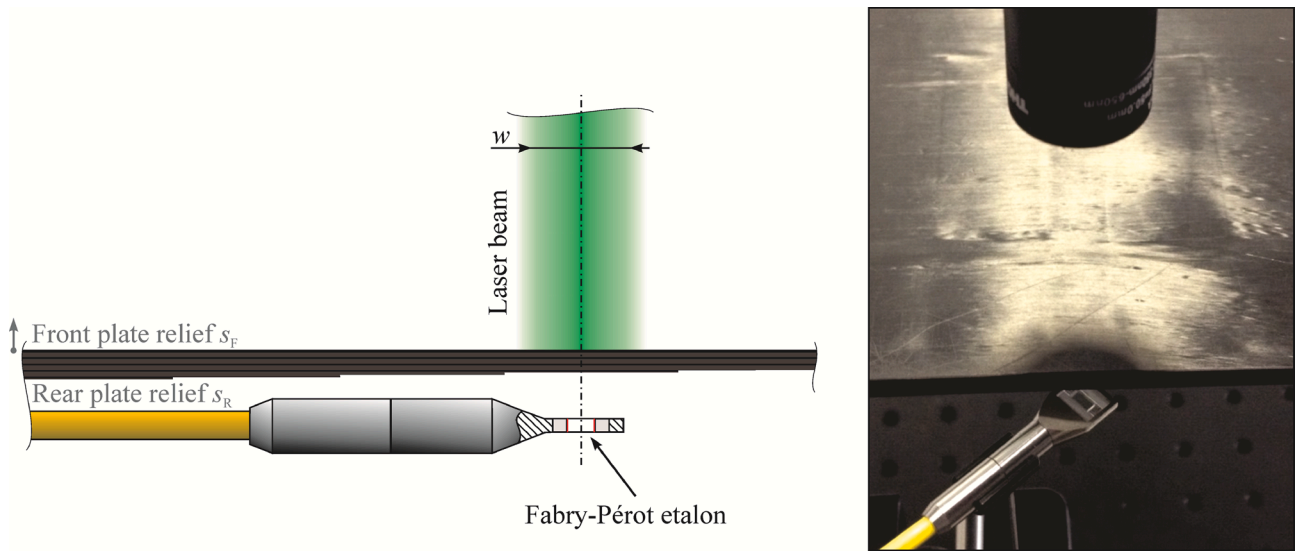


Fig. 2. Scheme and photo of the LURS experimental setup: US is excited by the pulse laser on the plain side of the plate. The local mechanical response of the plate is detected by the etalon of the optical microphone located on the opposite (rear) side of the plate.

min-long scan. The laser beam was driven simultaneously with the etalon over the 150×50 mm area of the CFRP plate, while inducing US pulses at 151×51 grid points (1-mm increment length). US acquisition using the optical microphone was externally triggered by the control unit at each of the scanning locations. No averaging was applied. The signal was digitalized using a 25-MHz sampling frequency and 14-bit encoder. A sufficient spatial resolution was achieved with an optical microphone aperture of 0.4-mm^2 as specified by the manufacturer. For supplementary details on the experimental setup, please refer to [19] or [24]. At the discrete thickness changes, the transition effect extended over one (rarely over two) scanning position. This indicates that the spatial resolution of our system was slightly higher than the increment length between two scanning grid points.

3. Theoretical relations

The reliefs of both plate surfaces can be expressed by the parameters TR frequency and ToA. They deliver two independent equations since US is generated on the specimen surface and detected in air. In the equation for the TR frequency

$$f_{TR} = \frac{v_M}{2(s_F - s_R)}, \quad (1)$$

the plate thickness can be expressed as a difference between the front s_F and the rear surface relief s_R in axial direction of the inspection system. v_M is the pressure wave velocity through the plate thickness.

ToA of the US generation on the front plate surface and its air-coupled detection on the opposite side of the plate is the sum of the travel time through the plate thickness and the detector-to-plate air gap:

$$t_{ToA} = \frac{s_F - s_R}{v_M} + \frac{s_R - D_{Ref}}{v_A}. \quad (2)$$

D_{Ref} is defined as a constant reference distance, which is dependent on the trigger delay and on the position of the US detector in the chosen coordinate origin, in which we describe the reliefs of the front and the rear plate surfaces. D_{Ref} is set to -4.6 mm for the coordinate origin on the topmost point of the front plate surface with the positive direction away from the plate. v_A is the pressure wave velocity in air during the experiment conditions: 343 m/s.

Inserting Eq. (1) to Eq. (2) and expressing the s_R yields

$$s_R = D_{\text{Ref}} + v_A \left(t_{\text{ToA}} - \frac{1}{2f_{\text{TR}}} \right) \quad (3)$$

The s_R (surface relief nearest to the air-coupled optical microphone) is independent of the plate material in a through-transmission setup since f_{TR} and t_{ToA} are both measurable in our experiment. Furthermore, the s_F (surface relief excited by the laser pulse) can be calculated from the s_R by addition of the plate thickness $s_F - s_R$, which can be obtained directly from the f_{TR} :

$$s_F = s_R + \frac{v_M}{2f_{\text{TR}}} = D_{\text{Ref}} + v_A \left(t_{\text{ToA}} - \frac{1}{2f_{\text{TR}}} \right) + \frac{v_M}{2f_{\text{TR}}}. \quad (4)$$

Thereby v_M , which affects the s_F measurement, needs to be known or measured at a reference point with known plate thickness.

4. Results and discussion

4.1. Typical signal

In Fig. 3, a typical signal recorded by the optical microphone is shown. The scanning point (100 mm, 25 mm) (scanning position x , scanning position y) lying between both grooves was chosen, where the plate had a thickness of 3.9 mm.

The epicentral normal displacement of the surface on the side of the plate opposite the laser excitation can be determined theoretically for given excitation parameters or by numerical simulation [7–9,20–22]. The normal epicentral displacement is reported to be a superposition of the displacements originating from the normal (e.g. driven by the ablation) and radial force distributions (driven by thermal expansion) when the laser pulse illuminates the plate surface. The normal force generates pressure waves, whilst the radial force generates shear waves, which propagate more slowly in the plate volume. The normal force causes bidirectional displacement with the first peak having a negative amplitude (named precursor). The positive direction is defined as away from the plate side opposite the excitation. The radial force induces a strictly positive normal displacement that follows the precursor. Radially oriented shear waves are converted to pressure waves on the plate side opposite the excitation.

The signal obtained by the optical microphone can be interpreted by comparing it to the theoretical epicentral normal displacement on the plate side opposite the excitation (rear side of the plate) described in the literature [7–9,20–22]. Despite the air gap between the plate's rear surface and the etalon, the waves that result from the pressure and shear waves in the plate can be identified in Fig. 3. The wave train begins with the negative precursor, which shows that the US was also partially induced by a normal force. With P, we mark the arrival of the direct pressure wave and with S, the shear wave that was converted to a pressure wave on the rear side of the plate. We also detect their two in-plate reflections (3P, 2PS, 5P and 4PS). The time difference between the pairs (P, 3P), (S, 2PS), (3P, 5P), and (2PS, 4PS) is constant at 2.8 μs , corresponding to the time it takes pressure waves to travel twice through

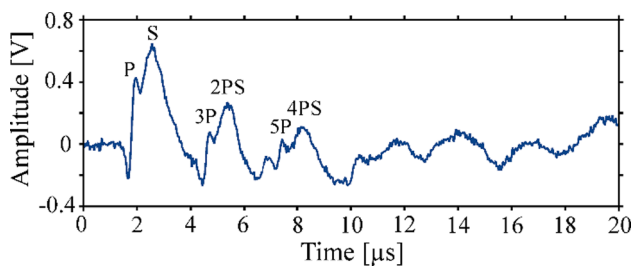


Fig. 3. A typical signal obtained by the optical microphone (A-Scan). The US was excited by a laser pulse at the location of full plate thickness. The waves which result from direct pressure and shear waves in the plate (P and S) and their reflections (3P, 2PS, 5P, 4PS) are marked.

the plate thickness. The resulting pressure wave velocity perpendicular to the fiber orientation is 2750 m/s, which agrees with the expected value for CFRP. The waves marked S, 2PS and 4PS arrive with approx. 1 μs delay relative to the waves P, 3P and 5P, respectively. This agrees with the expected delay caused by the different velocities of pressure and shear waves in solids [23].

4.2. B-Scans

In this section, we describe how the signal recorded by the optical microphone changes for various plate thicknesses. In Fig. 4 we show B-scans at scanning positions $y = 39$ mm (a) and $y = 9$ mm (b), which are marked in Fig. 1 with red lines. The thickness changes continuously in Fig. 4(a) and discretely in Fig. 4(b), as shown schematically in the cross-sections above the scans and described in the specimen description in Section 2 ‘Experimental Methods’.

Two parameters can be obtained from the signals for each of the scanning positions. The first parameter is ToA, which depends on the plate thickness and the air gap between the specimen and the etalon. The second one is the time difference between the first wave train (P and S wave) and subsequent reflections (3P, 2PS etc.), which carry the information about the plate thickness. Numerous in-plate reflections (from 5 to 20) detected, exhibit the high sensitivity of the setup used in this experiment. They can also be interpreted as through-thickness plate oscillations (symmetric Lamb waves). While the time arrival difference between the pressure and shear waves decreases as the plate thickness is reduced, the precursor shape (width of the first arriving wave) remains the same for all plate thicknesses. Due to this reason, the negative peak of the precursor was used to obtain a reliable ToA.

4.3. S-scans (B-scans in frequency domain)

For broadband LURS, the analysis in frequency domain B-scans (S-(spectrum) scans) is of particular interest. The Fourier transformation was applied to the time signal for all of the scanning positions. In Fig. 5 we show S-scans (B-scans in frequency domain) at scanning positions $y = 39$ mm (a) and $y = 9$ mm (b), which are marked in Fig. 1 with the red lines. Fig. 5 is Fig. 4 converted to the frequency domain. The amplitude range is expressed relative to the maximum TR peak amplitude.

The TR frequency has a higher amplitude than the higher-order resonance frequencies. It has a peak frequency at 330 kHz at the full plate thickness. The TR frequency increases as a multiplicative inverse function with linearly decreasing plate thickness (scanning positions x higher than 13 mm in Fig. 5(a)). The TR frequency peak, inversely proportional to the plate thickness, can also be observed in the S-scan when applied along the discrete groove (Fig. 5(b)). Higher-order resonance frequencies have a similar shape to that in TR, but a lower amplitude. The frequency components below 250 kHz are a consequence of the local resonances of the groove. These asymmetric oscillations become more pronounced for smaller plate thicknesses.

4.4. Determining the plate thickness

The periods of the in-plate reflections of the pressure waves were determined by inverting the TR peak frequencies for all scanning positions. In Fig. 6(a), these are displayed in grayscale-values. Assuming the homogeneity of the specimen, the periods of the in-plate reflections are directly proportional to the plate thicknesses, which can be easily obtained given the US pressure wave velocity perpendicular to the fiber orientation, or the plate thickness at a reference scanning location. We chose a point (150, 25) (scanning position x , scanning position y), where the thickness was measured with a dial gauge. The plate thicknesses scaled from the in-plate reflection periods are shown on the left side of the grayscale bar in Fig. 6.

The surface reliefs of the rear s_R and the front sides of the plate s_F obtained by Eq. (3) and (4) are shown in Fig. 6(b) and (c). The distances

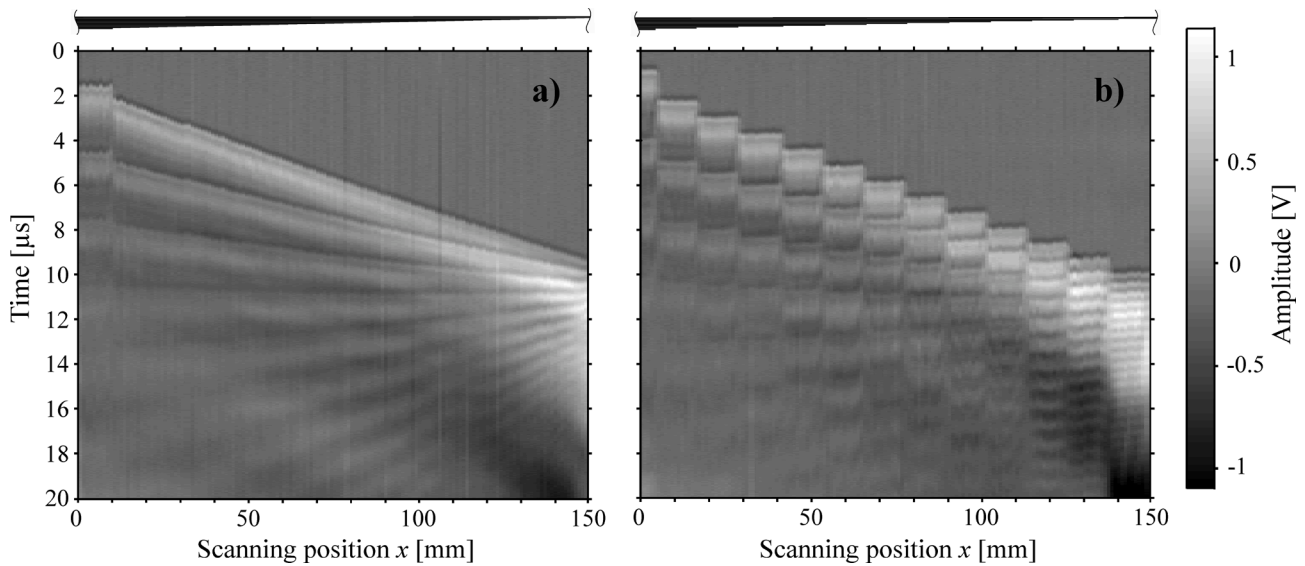


Fig. 4. B-scan over grooves with continuously (a) and discretely (b) changing thickness. The cross-sectional schemes above the scans show the thickness profile. The period of reflections and delay of S waves decrease as the plate thickness is reduced. The arrival time depends on the air gap between the specimen and the etalon.

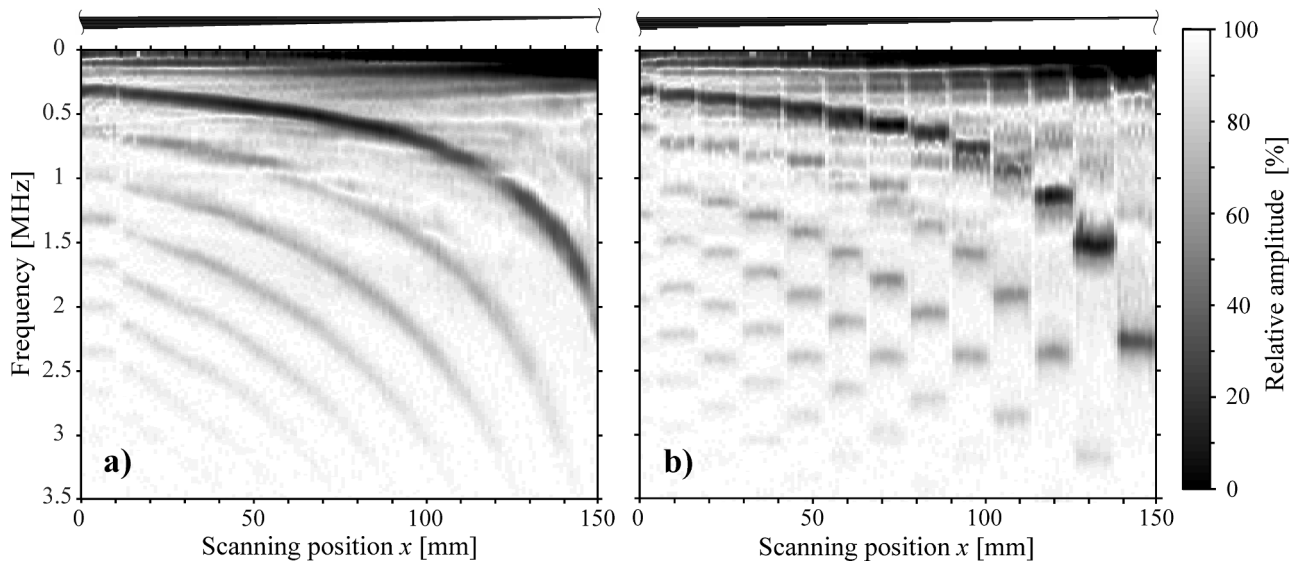


Fig. 5. S-scan (B-scan in frequency domain) over grooves with continuously (a) and discretely (b) changing thickness. The schemes above the scans show the thickness profile. The TR frequency is inversely proportional to the plate thickness and increases as a multiplicative inverse function with linearly decreasing plate thickness.

to the coordinate origin on the topmost point of the front plate surface (projected in the direction of the axis of the inspection system) are coded in grayscale.

The plate thickness profiles of the continuous and discrete grooves are clearly distinguished in Fig. 6(a). Furthermore, one can observe the change in the full plate thickness of the unmachined plate. It ranges from 3.6 mm (higher scanning position x) to 4.3 mm (lower scanning position x), as obtained via LURS. This variation is a consequence of inaccuracy of the manufacturing process and agrees with reference measurements of the geometrical thickness. A flat-bottom hole is located at (0 mm, 25 mm) (scanning position x , scanning position y), causing the shorter period of the in-plate reflections. Furthermore, at (45 mm, 50 mm), (98 mm, 50 mm) and (123 mm, 50 mm), variations in the period of in-plane reflections are visible. These are caused by simulated delaminations located there. They were created by placing pairs of polytetrafluoroethylene (PTFE) films between the carbon fiber layers during the

manufacturing process of the plate. An additional material-to-air interface attenuates high frequency components of the detected US. The delamination's local defect resonances with the lower modes can typically be detected below the TR frequency [3]. The delaminations can thus be easily distinguished from the thickness change, if the entire spectrum of the local mechanical response is analyzed. The only limitation is that the measurements of thickness and reliefs of the plate surfaces are not reliable at these locations, since the in-plate reflections are not easily detectable.

The s_R (Fig. 6(b)) can be obtained with high precision, since it is unaffected by the alteration of the plate material. In contrary, the s_F can be affected by change in the plate material or error of the TR frequency picking.

At discrete changes in the plate thickness or surface relief, the ToA can be picked before and the TR can be picked after the change (and vice versa). This can lead to an error that is especially observable in Fig. 6(b)

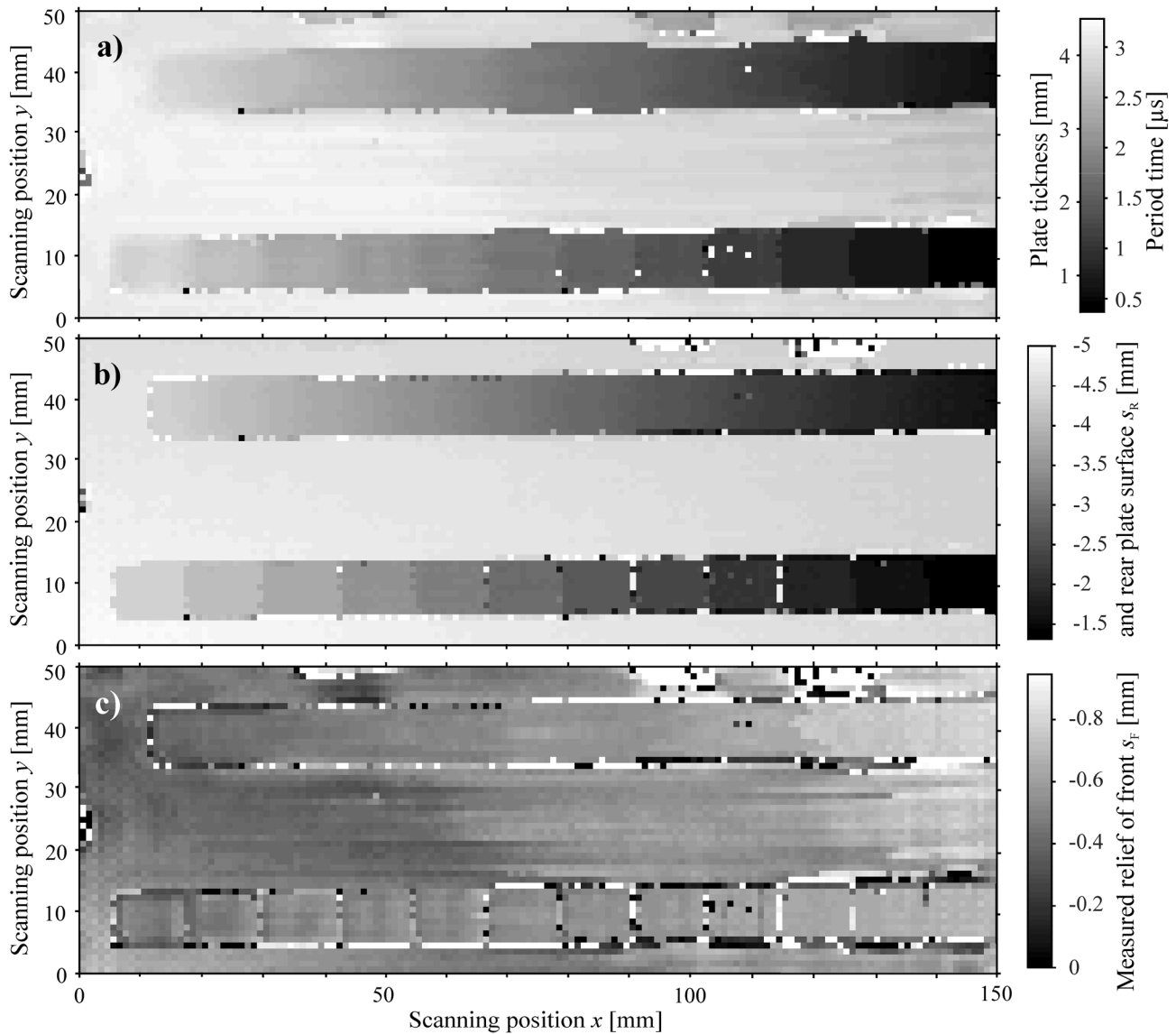


Fig. 6. Periods of in-plate reflections of the pressure waves, determined by inverting the TR frequency peak for all the scanning positions (a). The periods were scaled to the thicknesses of the plate using the geometrical thickness measured at the reference point. Measured reliefs of the rear s_R (b) and front plate surfaces s_F (c) were obtained by combining the measurements of TR and ToA using Eq. (3) and (4). Simulated delaminations are located at (45 mm, 50 mm), (98 mm, 50 mm) and (123 mm, 50 mm) (scanning position x , scanning position y). A flat-bottom hole is also visible at (0 mm, 25 mm).

as a frame formed around both grooves. However, the slope of the s_F is easily detectable outside as well as inside of the grooves.

To analyze the accuracy of the presented method, the measured thicknesses were compared to reference geometrical values, measured by the dial gauge. The measured thickness, lying between (inclusively) 35 mm and 41 mm scanning position y (central band of the continuous groove) is expected to be the same for a constant scanning position x . These seven values are gathered for each of the scanning positions x , and displayed by black dots in Fig. 7(a). The blue line represents the values of the geometrical thickness of the reference measurement. Data for the discrete groove is shown analogously. In Fig. 7(b) the measured values lying between (inclusively) 5 mm and 12 mm scanning position y are shown with black dots, and compared to the reference geometrical thickness measurement (blue line).

The measured slope of the continuous groove is slightly lower compared to the reference geometrical thickness. The scatter of the thickness determined by LURS is caused by the TR frequency peak picking imprecision and by the disturbances coming from the LURS setup. An increase of inaccuracy at a plate thickness of approximately

1.5 mm is due to the experimental setup; this disturbance at the corresponding frequency of 0.9 MHz is present independently of the plate thickness (Fig. 5). The outliers (above 4 mm thickness) come from the scanning points with the disturbed signal, for which the TR frequency peak was unable to be determined. They were excluded from the further analysis.

Certain deviations in the reference measurement (blue line in Fig. 7) of geometrical thickness can be a consequence of the measurement with the dial gauge or the machining process – e.g. nonlinearity of the continuous groove or non-equivalent step height for the discrete groove. Note that the blue line in Fig. 7 depicts the geometrical thickness, while the thickness measured by LURS can differ for the inhomogeneous material.

The reliefs of the rear s_R and the front plate surfaces s_F are shown in Fig. 8 at the same scanning positions as described above for Fig. 7. The s_R is obtained by Eq. (3) and the s_F by Eq. (4).

The surface relief measurement at the discrete groove has higher number of outliers, due to the discrete changes in the plate thickness.

A change in the plate thickness has a greater influence on the ToA

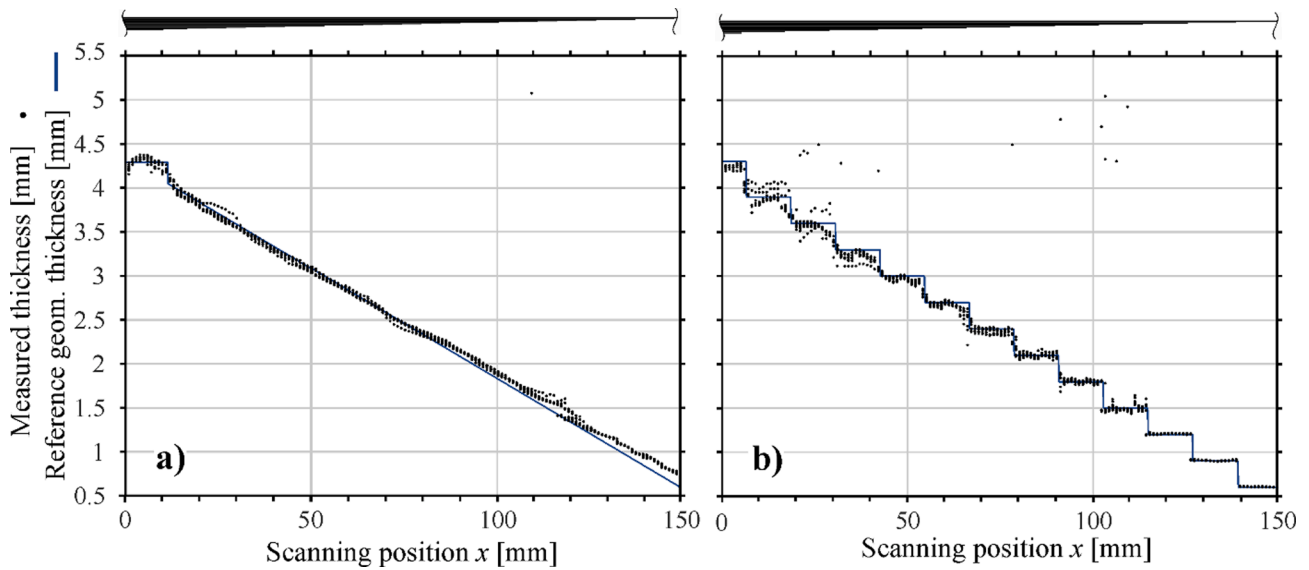


Fig. 7. The thicknesses measured by LURS (black dots) compared with the reference geometrical thickness (blue line). For each scanning position x , seven measured thicknesses (in the range between 35 mm and 41 mm scanning position y), which lie in the continuous groove (a) and eight measured thicknesses (in the range between 5 mm and 12 mm scanning position y), which lie in the discrete groove (b) are shown. The accuracy of the measurement improves for smaller plate thicknesses.

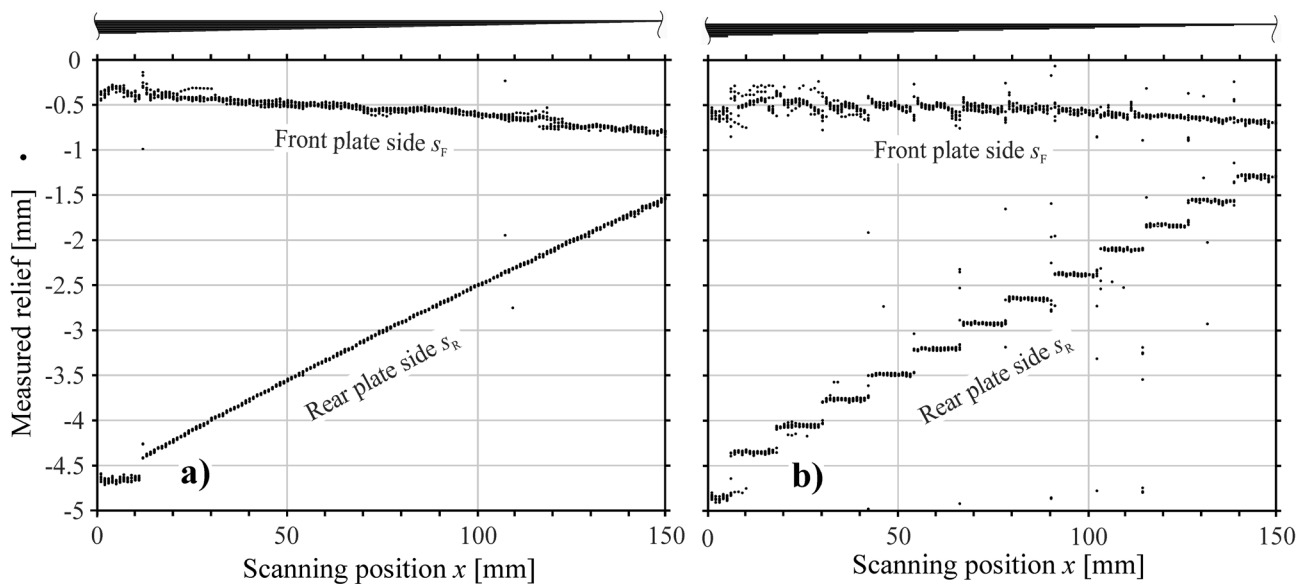


Fig. 8. The measured reliefs of the front s_F and the rear plate surfaces s_R for the same scanning positions as in Fig. 7: each scanning position x contains seven scanning positions y for continuous (a) and eight for discrete grooves (b). The accuracy of the s_F improves for smaller plate thicknesses, while the accuracy of s_R remains the same for all the measured plate thicknesses. s_F can be a potential indicator for the variations in the plate material properties, which, however, does not affect s_R .

than on the period of the in-plate reflections, because US velocity in air is approximately 8 times smaller than US velocity in the plate material. Consequently, the s_R has approximately the same accuracy for all of the plate thicknesses (standard deviation of approximately 13 μm). On the other hand, measurement accuracy of the plate thickness and of the s_F are strongly dependent on the plate thickness.

The following statistical analysis was performed in order to determine accuracy and precision of the thickness measurement. The measured thickness values of each plane of the discrete groove with the same thickness were gathered in groups. In the scanning coordinate system, these are located in the 10 mm \times 8 mm squares in the range between (inclusively) 5 mm and 12 mm (scanning position y). Each group contains 80 values, except the one at the full plate thickness, which contains 50 values. In Fig. 9, the mean values and standard

deviations of each group (normalization factor $N-1$, where N is the number of group elements) are expressed graphically and numerically and compared with the expected values obtained by the reference measurement. The smallest three thicknesses are shown in the exploded view in Fig. 9(b).

The standard deviation of the measured thickness decreases for smaller plate thicknesses due to the following reasons. TR frequency is inversely proportional to the plate thickness. Thus, the given change of thickness (0.3 mm in our case) has a bigger influence on TR frequency for small plate thicknesses. In other words, a 0.3-mm thickness decrement (our experiment), increases the TR frequency by approximately 8% at 3.9-mm plate thickness, while the last decrement (from 0.9 mm to 0.6 mm) increases the TR frequency by 50% (1.52–2.28 MHz). The error of the TR frequency peak picking is lower for thinner plate areas due to

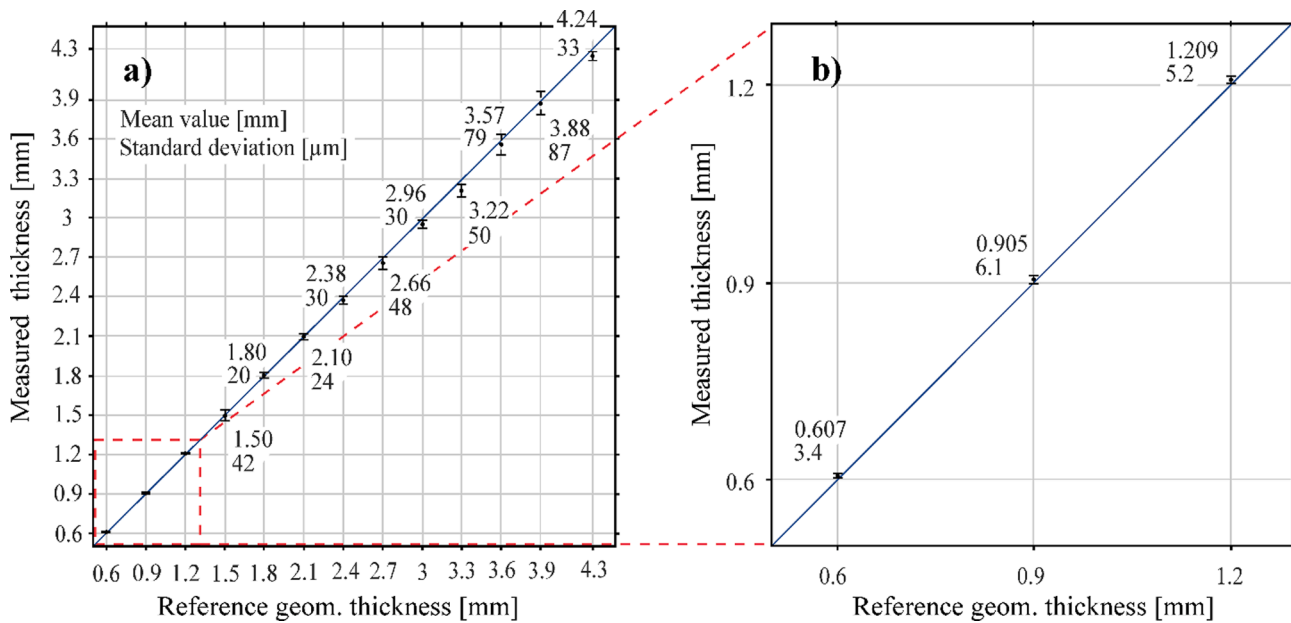


Fig. 9. Mean values and standard deviation for the thicknesses measured by LURS compared with the reference geometrical thicknesses. 80 values (50 for the full plate thickness) were evaluated for each thickness level of the discrete groove. The high-accurate results of the smallest three thicknesses are shown in the exploded view.

the following two reasons. Firstly, the relative error is smaller for higher TR frequencies. Secondly, more in-plate reflections can be captured for thinner plates (see Fig. 4(b)), which makes the TR peak more pronounced (see Fig. 5(b)). The extremely small measurement uncertainty of thicknesses below (inclusively) 1.2 mm is already close to the order of magnitude of the roughness of the surface. Note that the obtained thickness is averaged over the aperture size of the optical microphone.

LURS provides the thickness with a precision below the US wavelength in the plate, which amounts to 0.9 mm at 3 MHz testing frequency. The LURS approach can be interpreted as analogous to well-known phenomena of thin film interferometry of light, where interference conditions are highly sensitive to the film thickness and its refractive index. TR can be interpreted as an amplification of frequency components meeting the half-wavelength condition for constructive interference of US in the plate.

5. Conclusions

We described a new US broadband inspection method, termed LURS, which is able to determine the local mechanical properties of the specimen from the frequency spectrum of the local natural mechanical response. It was initiated by a novel experimental setup that is capable of effective generation and detection of US ranging from several kHz to several MHz.

In contrast to ACU methods, or methods where US is detected and generated on the specimen surface, air-coupled detection of US generated on the specimen surface delivers ToA and TR as two independent parameters. The reliefs of both plate surfaces (which contain the information about the plate curvature), together with the plate thickness, are obtained by a single scan in through-transmission setup. The measured relief of the plate surface excited by the laser and the measured plate thickness are influenced by changes in the plate material. The measured relief of the plate surface, which is turned toward the air-coupled optical microphone, remains unaffected.

We visualized the results over the scanned area containing continuous and discrete changes in the plate thickness. Statistical analysis was carried out. Thicknesses ranging from (inclusively) 0.6 mm to 1.2 mm were measured with a standard deviation of approximately 5 μm . The standard deviation increased with the plate thickness, but remained

below 100 μm for plate thicknesses below 4 mm.

Accuracy of the relief of the plate surface illuminated by the US excitation laser decreased for smaller plate thicknesses. On the other hand, accuracy of the relief of the plate surface closest to the US detector remained approximately the same for all of the plate thicknesses (standard deviation approximately 13 μm).

Delaminations in the plate material can be effectively detected by spectral analysis of the transmitted US. However, measurements of plate surface reliefs, thickness or plate material are not reliable there.

With the test on the plate of variable thicknesses, the sensitivity of the optical microphone was verified over the broadband frequency range. From the results (Fig. 5), it is apparent that the amplitude of the detected TR and high-order resonances remains approximately the same in the frequency range between 300 kHz and 3 MHz, except for a small disturbance at 900 kHz, which can also be a consequence of the US excitation system. Above 3 MHz, the sensitivity of the optical microphone decreases gradually. This frequency designates the limit of the method on plate thicknesses larger than approximately 0.4 mm for the material used (Eq. (1)). The maximum measurable thickness depends on the US attenuation level in the plate material, laser US excitation energy and sensitivity of the detector, which must allow the in-plate reflections to be visible.

The surface relief measurement of one side of plate can be detached from the material properties of the specimen by a joint analysis of TR and ToA. Reliefs of both plate surfaces, together with the mapped US velocity in the plate, could be obtained by applying a second scan with the reversed sides of the plate. This concept could be developed and turned into applications in which specimens with more complex geometry are scanned from different directions in order to reconstruct their shape together with their material properties. Acoustic tomography images could be reconstructed from signals obtained from differing positions of an ACU detector and laser excitation points on the specimen surface.

With the method described, it is possible to distinguish pressure and shear waves. A further goal of future work is to precisely determine pressure and shear wave velocities in the test material. The material inspection method will thus be improved to enable detection of the concrete local material parameters e.g. dynamic Young's and shear moduli.

Declaration of Competing Interest

The authors declare that they have no known competing financial interests or personal relationships that could have appeared to influence the work reported in this paper.

Acknowledgments

The authors acknowledge the Dr.-Ing. Otto and Karla Likar foundation for the financial support and XARION Laser Acoustics for providing the experimental equipment.

References

- [1] EN ISO 16809:2019 Non-destructive testing - Ultrasonic thickness measurement, BSI.
- [2] ASTM E797/E797M-15. Standard Practice for Measuring Thickness by Manual Ultrasonic Pulse-Echo Contact Method, ASTM International, West Conshohocken, PA, 2015, https://doi.org/10.1520/E0797_E0797M-15.
- [3] J. Rus, C.U. Grosse, Local ultrasonic resonance spectroscopy: a demonstration on plate inspection, *J. Nondestruct. Eval.* 39 (2) (2020) 31, <https://doi.org/10.1007/s10921-020-00674-5>.
- [4] W.M.D. Wright, D.A. Hutchins, Air-coupled ultrasonic testing of metals using broadband pulses in through-transmission, *Ultrasonics* 37 (1) (1999) 19–22, [https://doi.org/10.1016/S0041-624X\(98\)00034-1](https://doi.org/10.1016/S0041-624X(98)00034-1).
- [5] D.W. Schindel, D.A. Hutchins, Through-thickness characterization of solids by wideband air-coupled ultrasound, *Ultrasonics* 33 (1) (1995) 11–17, [https://doi.org/10.1016/0041-624X\(95\)00011-Q](https://doi.org/10.1016/0041-624X(95)00011-Q).
- [6] G. Waag, L. Hoff, P. Norli, Air-coupled ultrasonic through-transmission thickness measurements of steel plates, *Ultrasonics* 56 (2015) 332–339, <https://doi.org/10.1016/j.ultras.2014.08.021>.
- [7] R.J. Dewhurst, D.A. Hutchins, S.B. Palmer, C.B. Scruby, Quantitative measurements of laser-generated acoustic waveforms, *J. Appl. Phys.* 53 (4064) (1982) 4064–4071, <https://doi.org/10.1063/1.331270>.
- [8] D.A. Hutchins, Mechanisms of pulsed photoacoustic generation, *Can. J. Phys.* 64 (9) (1986) 1247–1264, <https://doi.org/10.1139/p86-217>.
- [9] S.J. Davies, C. Edwards, G.S. Taylor, S.B. Palmer, Laser-generated ultrasound: its properties, mechanisms and multifarious applications, *J. Phys. D Appl. Phys.* 26 (3) (1993) 329–348, <https://doi.org/10.1088/0022-3727/26/3/001>.
- [10] C.B. Scruby, L.E. Drain, *Laser Ultrasonics: Techniques and Applications*, A Hilger, Bristol, England, Philadelphia, 1990.
- [11] A. Moreau, D. Lévesque, M. Lord, M. Dubois, J.P. Monchalain, C. Padioleau, J. F. Bussière, On-line measurement of texture, thickness and plastic strain ratio using laser-ultrasound resonance spectroscopy, *Ultrasonics* 40 (10) (2002) 1047–1056, [https://doi.org/10.1016/S0041-624X\(02\)00255-X](https://doi.org/10.1016/S0041-624X(02)00255-X).
- [12] F.J. Shih, B.F. Pouet, M.B. Klein, A.D.W. McKie, Determination of glass thickness using laser-based ultrasound, *AIP Conf. Proc.* 557 (1) (2001) 287–292, <https://doi.org/10.1063/1.1373771>.
- [13] J.D. Ausseil, J.P. Monchalain, Precision laser-ultrasonic velocity measurement and elastic constant determination, *Ultrasonics* 27 (3) (1989) 165–177, [https://doi.org/10.1016/0041-624X\(89\)90059-0](https://doi.org/10.1016/0041-624X(89)90059-0).
- [14] M. Perterer, *Schadensidentifikation und -bewertung von CFK-Bauteilen mittels phasenmodulierter Thermographie*, Dissertation, Technical University of Munich, 2012.
- [15] B. Fischer, Optical microphone hears ultrasound, *Nat. Photonics* 10 (2016) 356–358, <https://doi.org/10.1038/nphoton.2016.95>.
- [16] S. Preisser, W. Rohringer, M. Liu, C. Kollmann, S. Zotter, B. Fischer, W. Drexler, All-optical highly sensitive akinetic sensor for ultrasound detection and photoacoustic imaging, *Biomed. Opt. Express* 7 (10) (2016) 4171–4186, <https://doi.org/10.1364/BOE.7.004171>.
- [17] S. Preisser, B. Fischer, N. Panzer, Listening to ultrasound with a laser, *Opt. Photon.* 12 (5) (2017) 22–25, <https://doi.org/10.1002/opph.201700031>.
- [18] B. Fischer, F. Sarasini, J. Tirillò, F. Touchard, L. Chocinski-Arnault, D. Mellier, N. Panzer, R. Sommerhuber, P. Russo, I. Papa, V. Lopresto, R. Ecault, Impact damage assessment in biocomposites by micro-CT and innovative air-coupled detection of laser-generated ultrasound, *Compos. Struct.* 210 (2019) 922–931, <https://doi.org/10.1016/j.compstruct.2018.12.013>.
- [19] J. Rus, B. Fischer, C.U. Grosse, Photoacoustic inspection of CFRP using an optical microphone, *Proc. SPIE, Optical Measurement Systems for Industrial Inspection XI1105622* (2019), <https://doi.org/10.1117/12.2525021>.
- [20] J. Laloš, T. Požar, J. Možina, Transition from 1D to 2D laser-induced ultrasonic wave propagation in an extended plate, *Int. J. Thermophys.* 37 (5) (2016) 1–10, <https://doi.org/10.1007/s10765-016-2056-y>.
- [21] A.G. Every, Z.N. Utegulov, I.A. Veres, Laser thermoelastic generation in metals above the melt threshold, *J. Appl. Phys.* 114 (20) (2013), 203508, <https://doi.org/10.1063/1.4832483>.
- [22] J. Laloš, M. Jezeršek, R. Petkovšek, T. Požar, Laser-induced ultrasonic waveform derivation and transition from a point to a homogeneous illumination of a plate, *Ultrasonics* 81 (2017) 158–166, <https://doi.org/10.1016/j.ultras.2017.06.018>.
- [23] K.F. Graff, *Wave Motion in Elastic Solids*, Dover Publications, New York, 1991.
- [24] J. Rus, A. Gustschin, H. Mooshofer, J.C. Grager, K. Bente, M. Gaal, F. Pfeiffer, C. U. Grosse, Qualitative comparison of non-destructive methods for inspection of carbon fiber-reinforced polymer laminates, *J. Compos. Mater.* (2020), <https://doi.org/10.1177/0021998320931162>.